International Journal of Nanomedicine

Dovepress
open access to scientific and medical research

Open Access Full Text Article

ORIGINAL RESEARCH

Dual targeting curcumin loaded alendronate-hyaluronan- octadecanoic acid micelles for improving osteosarcoma therapy

This article was published in the following Dove Press journal:
International Journal of Nanomedicine

Yanhai Xi,[1,*] Tingwang Jiang,[2,*] Yinglan Yu,[3] Jiangmin Yu,[1] Mintao Xue,[1] Ning Xu,[1] Jiankun Wen,[1] Weiheng Wang,[1] Hailong He,[1] Yan Shen,[3] Daquan Chen,[4] Xiaojian Ye,[1] Thomas J Webster[5]

[1]Department of Spine Surgery, Changzheng Hospital, Second Military Medical University, Shanghai, People's Republic of China; [2]Department of Immunology and Microbiology, Institution of Laboratory Medicine of Changshu, Changshu 215500, Jiangsu, People's Republic of China; [3]Department of Pharmaceutics, Center for Research Development and Evaluation of Pharmaceutical Excipients and Generic Drugs, China Pharmaceutical University, Nanjing, People's Republic of China; [4]Department of Pharmaceutics, School of Pharmacy, Yantai University, Yantai 264005, People's Republic of China; [5]Department of Chemical Engineering, Northeastern University, Boston, MA, USA

*These authors contributed equally to this work

Correspondence: Xiaojian Ye
Department of Spine Surgery, Changzheng Hospital, Second Military Medical University, Shanghai 200003, People's Republic of China
Tel +86 1 381 734 6934
Email xjyespine@smmu.edu.cn

Thomas J Webster
Department of Chemical Engineering, Northeastern University, 360 Huntington Avenue, Boston, MA 02115, USA
Tel +1 617 373 6585
Email th.webster@neu.edu

Introduction: Curcumin (CUR) is a general ingredient of traditional Chinese medicine, which has potential antitumor effects. However, its use clinically has been limited due to its low aqueous solubility and bioavailability. In order to improve the therapeutic effect of CUR on osteosarcoma (i.e., bone cancer), a multifunctional micelle was developed here by combining active bone accumulating ability with tumor CD44 targeting capacity.

Methods: The CUR loaded micelles were self-assembled by using alendronate-hyaluronic acid-octadecanoic acid (ALN-HA-C18) as an amphiphilic material. The obtained micelles were characterized for size and drug loading. In addition, the in vitro release behavior of CUR was investigated under PBS (pH 5.7) medium containing 1% Tween 80 at 37℃. Furthermore, an hydroxyapatite (the major inorganic component of bone) affinity experiment was studied. In vitro antitumor activity was evaluated. Finally, the anti-tumor efficiency was studied.

Results: The size and drug loading of the CUR loaded ALN-HA-C18 micelles were about 118 ± 3.6 nm and 6 ± 1.2%, respectively. CUR was released from the ALN-HA-C18 micelles in a sustained manner after 12 h. The hydroxyapatite affinity experiment indicated that CUR loaded ALN-HA-C18 micelles exhibited a high affinity to bone. CUR loaded ALN-HA-C18 micelles exhibited much higher cytotoxic activity against MG-63 cells compared to free CUR. Finally, CUR loaded ALN-HA-C18 micelles effectively delayed anti-tumor growth properties in osteosarcoma bearing mice as compared with free CUR.

Conclusion: The present study suggested that ALN-HA-C18 is a novel promising micelle for osteosarcoma targeting and delivery of the hydrophobic anticancer drug CUR.

Keywords: curcumin, alendronate, hyaluronic acid, osteosarcoma

Introduction

Curcumin (CUR, diferuloylmethane) is a naturally occurring polyphenolic phytochemical derived from the rhizome of the herb *Curcuma longa L*, which has a wide spectrum of biological and pharmacological activities.[1] The potential antitumor effect of curcumin has attracted extensive attention, and a lot of research has been conducted in this field.[2–4] However, the major challenge of CUR is its poor solubility in an aqueous solution (~20 μg/mL) and its poor bioavailability, which limits its clinical application.[5] In order to improve its aqueous solubility and bioavailability, substantial attempts have been made through encapsulation in polymeric micelles, nanoparticles, liposomes, and hydrogels.[6–9] Among these approaches, an attractive alternative method for addressing its low aqueous solubility is to encapsulate CUR in

polymeric micelles, and several researchers have shown that CUR has a significantly higher solubility in surfactant micelle solutions.[10,11] However, the use of these formulations has been further limited by a lack of selectivity and high toxicity to normal cells.

Among polymeric micelles, hydrophobic polysaccharides have currently become one of the most popular research areas in the field of drug delivery nanoparticles. Hyaluronic acid (HA) is a natural linear polysaccharide composed of N-acetyl-D-glucosamine and D-glucuronic acid, which has a strong affinity with cell-specific surface markers, such as a receptor for HA-mediated motility (RHAMM) and glycoprotein CD_{44}.[12] Tumor cells with high metastatic activities often exhibit enhanced binding and uptake of HA, due to HA receptors (RHAMM and CD44) overexpressed on the tumor cell surface.[13,14] Thus, substantial studies have focused on using the tumor targeting potential of HA for antitumor therapeutic agent delivery.[15,16] However, because of its high hydrophilicity, free HA biopolymers can be incompatible with innovative applications towards the encapsulation and selective delivery of drugs. In this study, hydrophilic HA and hydrophobic octadecanoic acid were linked by ester bonds to form the amphiphilic copolymer hyaluronic acid-octadecanoic acid (HA-C_{18}), which can form stable micelles.

Osteosarcoma is a common primary type of malignant bone cancer in children and young adults between 10 and 20.[17,18] On the other hand, osteosarcoma is a very aggressive cancer, associated with poor prognosis.[19] For children and adolescents, osteosarcoma most frequently occurs in developing bones, resulting in metastases in the lungs and subsequent failure of the respiratory system.[20,21] Bisphosphonates (BPs) show strong affinity with hydroxyapatite, which is the main mineral component of bone. Therefore, BPs can selectively accumulate in bone and target osteosarcoma for drug delivery applications.[22] Alendronate (ALN) is a new amino bisphosphonate, which is commonly used for treating bone related diseases and can be used as a bone targeting ligand.[23,24] So in this work, to improve the selectively of agents to osteosarcoma tissue, ALN was used to modify HA-C_{18} micelles.

In this research, in order to enhance the therapeutic effect of curcumin on osteosarcoma, alendronate-hyaluronic acid-octadecanoic acid (ALN-HA-C_{18}) was prepared. The copolymer could then self-assemble into micelles, and free curcumin could be encapsulated into the micelle. The critical micelle concentration (CMC) of the micelles was investigated. In addition, the drug release of the CUR loaded ALN-HA-C_{18} micelles and the binding affinity of the CUR loaded ALN-HA-C_{18} micelles with hydroxyapatite were evaluated. Finally, the in vitro cytotoxicity and in vivo anticancer effect of CUR loaded ALN-HA-C_{18} micelles were further analyzed.

Materials and methods

Materials

Oligosaccharides of hyaluronan (HA) (molecular weight [MW] <10 kDa) was purchased from Shandong Freda Co., Ltd. (Shandong, China). Alendronate (ALN) was the product of Shanghai Huacheng Industrial Development Co., Ltd. (Shanghai, China). Octadecanoic acid was the product of Sinopharm (Beijing, China). Curcumin (CUR), 4-Dimethylaminopyridine (DMAP), 1-ethyl-(3-dimethylaminopropyl) carbodiimide hydrochloride (EDC), and N-Hydroxysuccinimide (NHS) were obtained from Aladdin (Shanghai, China). N, N'-Dicyclohexyl Carboimide (DCC) was supplied by China Pharmaceutical Group Chemical Reagents Co., Ltd. (Shanghai, China). Dimethyl sulfoxide (DMSO) was offered by Tianjin Bodi Chemical Co., Ltd. (Tianjin, China). Acetonitrile (HPLC grade, 99.9%) was supplied by Beijing Brilliant Technology Co., Ltd. (Beijing, China). Fetal bovine serum (FBS), DMEM, coumarin-6 (C6), 4,6-diamidino-2-phenylindole (DAPI), 4% paraformaldehyde and 3-(4,5-dimethyl-thiazol-2-yl)-2,5-diphenyl-tetrazolium bromide (MTT) were purchased from Saiersi Biotechnology Co. Ltd. (Shangdong, China). All reagents were of commercial grade. The water used in the experiments was deionized water.

MG-63 osteosarcoma cells and healthy human osteoblast (HOB) cells were used in our study. HOB cells were purchased from Lonza® (Basel, Switzerland, Number: CC-2538) and cultured in a 37 °C, 5% CO_2 environment in a mixed medium consisting of Osteoblast Basal Medium (Promocell, Heidelberg, Germany) supplemented with 10% Osteoblast Supplement Mix (Promocell, Heidelberg, Germany), and 1% Penicillin-Streptomycin (Sigma-Aldrich, St. Louis, Missouri, USA). MG-63 cells were purchased from Nanjing Keygen Biotech Co., Ltd. (Nanjing, China, KG231) and cell experiments were approved by the China Pharmaceutical University review board. The MG-63 cells were cultured in DMEM medium (Gibco, Invitrogen, Carlsbad, Calif., USA), containing 10% (v/v) fetal bovine serum and 100 U/mL penicillin and 100 μg/mL streptomycin sulfate in a 37 °C, 5% CO_2 environment. The use of the cell lines was approved by the ethics committee of the China Pharmaceutical University.

Female nude mice weighing 14–18 g (3–4 weeks) were supplied by Beijing Vital River Laboratory Animal Technology Co., Ltd. (Beijing, China). All experimental protocols were approved by the China Pharmaceutical University Animal Experiment Center and followed the principles of laboratory and animal care of the university.

Synthesis and characterization of the ALN-HA-C_{18} polymer

The HA-C_{18} material was synthesized via an esterification reaction and the synthetic routes are shown in Figure 1A. Firstly, octadecanoic acid was activated by EDC and DMAP in DMSO for 2 h at 80 °C. Then, HA was dissolved in deionized water, and the above reaction solution was dropped into it and the reaction mixture was stirred for 12 h at 45 °C. The reaction mixture was completely dialyzed in deionized water and lyophilized (LGJ-10FD, Beijing Songyuanhuaxing Technology Develop Co., Ltd, China) to obtain the HA-C_{18} polymer. The content of octadecanoic acid in the polymer was determined by ^{1}H-NMR.

ALN was conjugated with a HA-C_{18} by amino bond as shown in Figure 1B. In brief, the HA-C_{18} was dissolved in deionized water, and the pH of the solution was adjusted to pH 2–3 by dropwise adding a 1 mol/L hydrochloric acid solution. The acidic HA-C_{18} solution was activated by EDC and NHS at 60 °C for 1 h. Then, ALN was dissolved in deionized water and dropped into the above reaction mixture, and the reaction mixture was stirred for 12 h at 45 °C. Finally, the reaction mixture was dialyzed in deionized water and lyophilized to obtain an ALN-HA-C_{18} conjugate. The content of ALN in the ALN-HA-C_{18} polymer was calculated by potentiometric titration with a sodium hydroxide titration solution using the ALN unmodified HA-C_{18} polymer as a reference.

The composition and the structure of each copolymer were determined using a 300 MHz ^{1}H-NMR (BRUKER AV-500, Germany). HA was dissolved in D_2O and the amphiphilic material ALN-HA-C_{18} was dissolved in D_2O: DMSO-D_6 (1: 1, v/v) for further measurements.

The critical micelle concentration (CMC) of the ALN-HA-C_{18} polymer

The CMC of the ALN-HA-C_{18} polymer was determined by pyrene as a fluorescence probe.[25] Firstly, pyrene was dissolved in acetone and the acetone was fully evaporated. Then, different concentrations of ALN-HA-C_{18} solutions ranging from 1.0×10^{-4} to 5.0×10^{-1} mg/mL were added into the pyrene. Finally, these solutions were sonicated (SK250HP, Shanghai Kedao Ultrasound Instrument Co., Ltd., China) for 30 min and then kept at room temperature overnight by avoiding light to reach equilibrium before fluorescence measurements.

The fluorescence spectra solutions were recorded by a fluorescence spectrometer (Lumina, Thermo Fisher, Massachusetts, USA). The excitation wavelength was fixed at 336 nm and the emission spectrum was recorded from 360 nm to 450 nm. The CMC of ALN-HA-C_{18} was indicated by the crossover points in the plots of the fluorescence intensity ratio of the first peak (I_1, 373 nm) and the third peak (I_3, 384 nm) to the logarithm concentration.

Preparation of CUR loaded ALN-HA-C_{18} micelles

The CUR loaded ALN-HA-C_{18} micelles were prepared by the film dispersion method. Briefly, the ALN-HA-C_{18}

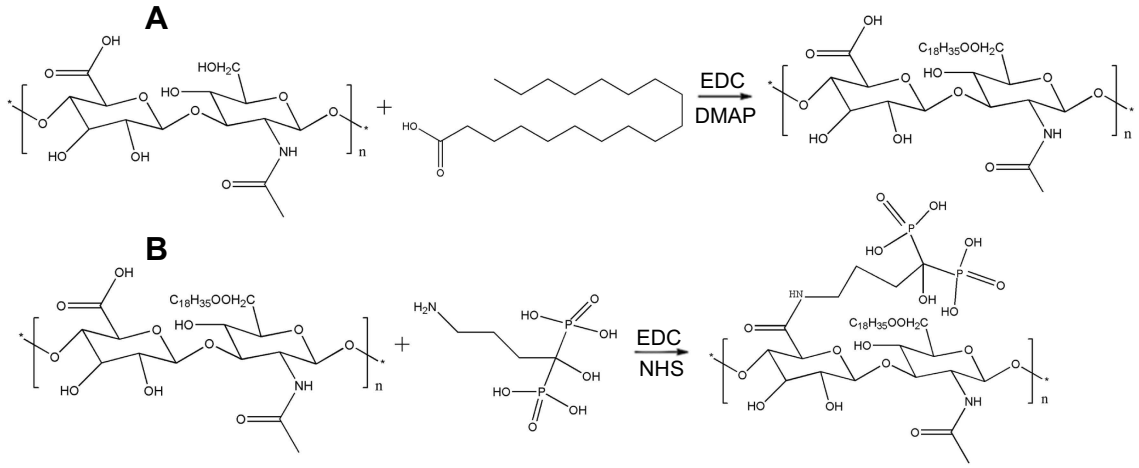

Figure 1 Schematic representation for the synthesis of (**A**) hyaluronic acid-octadecanoic acid (HA-C_{18}) and (**B**) alendronate-hyaluronic acid-octadecanoic acid (ALN-HA-C_{18}).

polymer and CUR were dissolved into absolute ethanol. After that, the organic content from the mixture was completely removed by a vacuum rotary evaporator at 40 °C. The dried film in the bottle was consolidated at 80 °C for 10 mins. Finally, the micelle film was dispersed in deionized water and the solution was centrifuged (KDC-140HR, Anhui Zhongke Zhongjia Scientific Instruments Co., Ltd., China) at 3000 rpm for 15 min to remove the unloaded CUR. The solution was filtered through a 0.22 μm millipore membrane (Tianjin Jinteng Experimental Equipment Co., Ltd., Tianjin, China) and the expected yellow CUR micelle solution was obtained.

Optimization of the preparation process

In order to optimize the preparation process, an orthogonal design was used based on single factor experiments. The particle size (Y_1) and entrapment efficiency (EE%, Y_2) were taken as the indicators to choose the best technology. The three independent variables are the mass ratio of polymer to drug (X_1), type of organic solvent (X_2), and solidification temperature (X_3). The independent variables and dependent variable responses are listed in Table 1.

Characterization of CUR loaded ALN-HA-C_{18} micelles

Particle size and size distribution

The average particle size and size distribution of the CUR loaded ALN-HA-C_{18} micelles were measured by dynamic light scattering (DLS) using a Delsa Nano C Nanometer Particle Size Meter (Beckmann, California, USA). All measurements were performed at room temperature and the data were obtained from the mean of three measurements.

Transmission electron microscopy (TEM)

A drop of the CUR loaded ALN-HA-C_{18} micelle solution with a concentration of 0.5 mg/mL was attached to the copper network and was mixed with a drop of 2% (w/v) phosphotungstic acid followed by drying in air. The morphology of the CUR loaded ALN-HA-C_{18} micelle was examined by a JEM-1400 transmission electron microscope (Jeol, Tokyo, Japan) using standard protocols.

Measurement of CUR concentrations in the micellar solution

The concentration of CUR in the micellar solution was measured by High Performance Liquid Chromatography (HPLC, Agilent, California, USA). The mobile phase consisted of acetonitrile and 0.5% acetic acid (60: 40, v/v). The Inertsil® ODS-SP column (4.6×250 mm, 5 μm, Shimadzu, Tokyo, Japan) was used. The flow rate was 1.0 mL/min, the detection wavelength was 425 nm with the UV detector, the column temperature was 25 °C and the injected volume of the sample solution was 20 μL.

Determination of drug entrapment efficiency (EE%) and drug loading (DL%)

Two milliliters of a CUR loaded ALN-HA-C_{18} micellar solution was diluted with methanol and treated with ultrasonication for 3 min, followed by diluting with methanol to 10 mL. After being filtered with a 0.22 μm microfiltration membrane, the content of CUR was determined by the HPLC method. The EE% was assayed as the percentage of the drug amount incorporated in the micelles of the total drug amount added in the solution. On the other hand, the DL% was calculated as the ratio of the drug amount in the micelles to the total amount of the micelles.

In vitro release study

Release of CUR from CUR loaded ALN-HA-C_{18} micelles was determined by the dialysis method. Firstly, phosphate buffered saline (PBS, 40 mL) at pH 5.7 containing 1% Tween 80, was employed as the release medium. 2 mL of the CUR solution (1 mg/mL, DMF-polyethylene glycol 400–5% glucose solution, v/v/v, 15: 45: 40) and 2 mL of the CUR loaded ALN-HA-C_{18} micelles (1 mg/mL) were placed in a dialysis bag, respectively. Then, the dialysis bags were immersed in the medium and followed by shaking at a speed of 100 rpm/min at 37 °C. At predetermined time intervals, 2 mL aliquots of the medium were withdrawn and the same volume of fresh

Table 1 The orthogonal design factors and levels

Independent variables	Levels		
	1	2	3
X_1: The mass ratio of polymer to drug	5: 1	10: 1	15: 1
X_2: Type of organic solvent	Ethanol	Acetone	Chloroform
X_3: Solidification temperature (°C)	40	60	80

medium was added. Finally, the in vitro release behavior of the CUR loaded micelles was measured by HPLC. All assays were performed in triplicate.

Hydroxyapatite affinity assay

To evaluate the affinity to hydroxyapatite, CUR, CUR loaded HA-C_{18} micelles and CUR loaded ALN-HA-C_{18} micelles (2 mL, 0.5 mg/mL) were added into a 8 mL PBS solution separately. Then, 100 mg of hydroxyapatite was dispersed into the solution and gently shaken at room temperature. At the same time, CUR, CUR loaded HA-C_{18} micelles and CUR loaded ALN-HA-C_{18} micelles were respectively incubated at the same condition without hydroxyapatite as the control. After 1 h, the mixture solution was centrifuged (4000 rpm, 10 min) and the absorbance of the supernatant (diluted with the same volume methanol) was measured by a UV-1800 Ultraviolet-Visible (UV-Vis) spectrophotometer (Shimadzu, Tokyo, Japan) at 425 nm. The binding percentage with hydroxyapatite was calculated as the ratio of the difference between the control group and the test group to the control group.

In vitro cytotoxicity assay

The in vitro cytotoxicity of CUR loaded ALN-HA-C_{18} micelles was evaluated on MG-63 osteosarcoma cells and healthy human osteoblast (HOB) cells using the MTT method. In brief, the cell lines were seeded at a density of 5×10^3 cells per well in 96-well plates. After a 24 h incubation, 200 μL of medium was added containing the treatment agents which were the free CUR DMSO solution (the final concentration of DMSO was kept below 0.2%), blank micellar solutions and CUR loaded ALN-HA-C_{18} micelle solutions of various concentrations. The final concentrations of CUR were 1.25, 2.5, 5, 10, 20, and 40 μM. After an additional 48 h of incubation, 20 μL of MTT (5 mg/mL) was added and incubated for another 4 h at 37 °C. The medium was removed and the intracellular metabolized product formazan crystals were dissolved by the addition of 150 μL of DMSO to each well. The absorbance was measured using a ELx800 microplate reader (BioTek, Vermont, USA) with the test wavelength at 570 nm. Untreated cells were taken as a control with 100% viability and cells without the addition of MTT were used as blanks to calibrate the spectrophotometer to a zero absorbance. The relative cell viability (%) was calculated as: (OD of treated cells - OD of blank)/(OD of nontreated cells - OD of blank) ×100%.

Cellular uptake of micelles

Inverted fluorescence microscope and flow cytometry were used to investigate the cellular uptake of the C6-loaded ALN-HA-C_{18} micelles. For inverted fluorescence microscope experiments, the MG-63 osteosarcoma cells were seeded into 6-well plates at a density of 1×10^5 cells per well and were cultured overnight at 37 °C. Then, the cell culture medium was replaced with serum-free cell culture medium containing free C6, C6-loaded ALN- HA-C_{18} micelles with HA and C6-loaded ALN- HA-C_{18} micelles (the equivalent C6 concentration: 100 ng/mL) and was incubated for 4 h at 37 °C, respectively. Then, the cells were slightly rinsed with cold PBS for three times and fixed with 4% paraformaldehyde. Finally, the cells were slightly rinsed with cold PBS for three times and treated with DAPI (100 ng/mL) for 10 min to stain the nucleus. The cells were rinsed with cold PBS for three times and observed by an Olympus IX53 inverted fluorescence microscope (Olympus Corporation, Tokyo, Japan).

For flow cytometry, the MG-63 osteosarcoma cells were seeded in 6-well plates at a density of 1×10^5 cells per well and were cultured overnight at 37 °C. Then, the cells were incubated with free C6, C6-loaded ALN-HA-C_{18} micelles with HA and C6-loaded ALN-HA-C_{18} micelles (the equivalent C6 concentration: 100 ng/mL) at 37 °C for 4 h. The cells were digested by trypsin. The suspensions were centrifuged at 1000 rpm/min for 3 min, washed twice with PBS, and then re-suspended in 0.5 mL of PBS. Finally, making use of a flow cytometer (MACSQuantTM, Miltenyl Biotec, Germany) with an excitation wavelength at 488 nm and an emission wavelength at 530 nm, we measured the fluorescent intensity of the cells.

In vivo antitumor activity

The antitumor activity of CUR loaded ALN-HA-C_{18} micelles in vivo was evaluated in an osteosarcoma model employing nude mice. The MG-63 osteosarcoma cells (1×10^8 cells/mice) were injected into the right tibia of male nude mice. After 12 days of tumor cell inoculation, mice were randomized in three different groups and treated with saline, free CUR (25 mg/kg), CUR loaded HA-C_{18} micelles (25 mg/kg) and CUR loaded ALN-HA-C_{18} micelles (25 mg/kg), respectively. Treatment was carried out every other day by tail vein injection for 20 days. During the administration, the long diameter (length) and the short diameter (width) of the tumors were measured with a caliper every 2 days. The tumor volume was calculated by using the formula: volume =

length × width^2/2. At the end of the study period, the mice were sacrificed. The organs, including the heart, liver, spleen, lung and kidney, were resected and stored in 10% formalin solution (v/v) at 4 °C. Then, the tissues were embedded in paraffin and stained with hematoxylin and eosin (H&E).

Statistical analysis

The data were analyzed using SPSS software, version 19. Statistical comparisons were performed by one way ANOVA for different groups. Significant differences between or among groups are indicated by $*P<0.05$, $**P<0.01$ and $***P<0.001$. Experiments were done in triplicate. The results are expressed as the mean ± standard deviation (SD).

Results and discussion

Polymer synthesis and characterization

The ALN-HA-C_{18} material was synthesized via a series of esterification reactions. The ^{1}H NMR spectra of HA and ALN-HA-C_{18} are shown in Figure 2. As shown in the ^{1}H NMR spectrum of HA, the N-acetyl (-$NHCOCH_3$) peak can be identified at δ (ppm) 1.95 along with glucosidic H (10 H) at δ (ppm) 3.0–4.0 and anomeric H (2 H) at δ (ppm) 4.45 and 4.55. Compared with HA, the ^{1}H NMR spectrum of ALN-HA-C_{18} showed new emergent peaks at δ (ppm) 1.05 and 1.25, belonging to the signals of the methyl (-CH_3) and the methylenes (-CH_2-) of the long chain octadecyl group, respectively. The results confirmed the successful conjugation of an octadecyl group onto the HA backbone. Moreover,

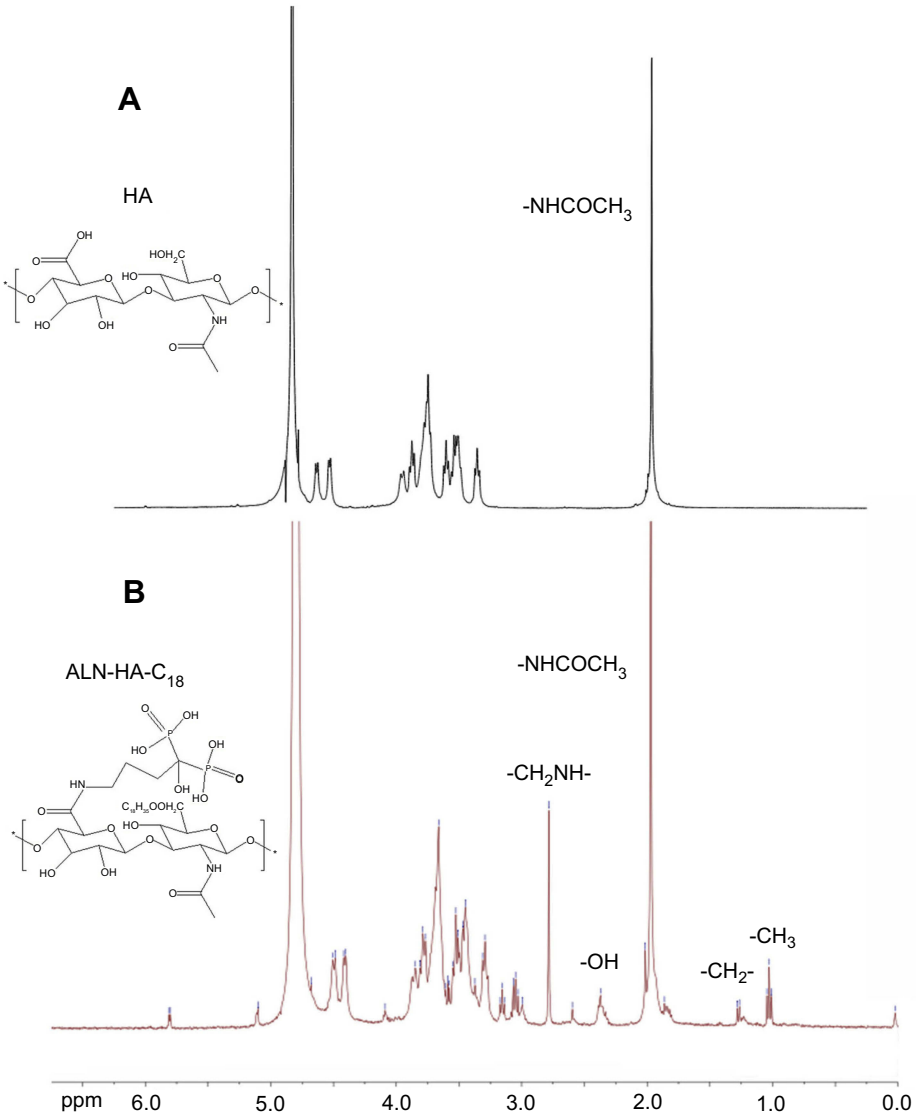

Figure 2 ^{1}H NMR spectrum of (**A**) hyaluronic acid (HA) and (**B**) alendronate-hyaluronic acid-octadecanoic acid (ALN-HA-C_{18}).

the ALN in ALN-HA-C_{18} was verified by the signals at peak δ (ppm) 2.75 and 2.3, which are the peaks of -CH_2NH and -C(OH)[$PO(OH)_2$]$_2$, respectively.

The degree of substitution (DS) was defined as the number of octadecyl groups per 100 sugar residues of the HA-C_{18} conjugate. To determine the DS of the octadecyl group to HA, the relative intensity ratio of the -$NHCOCH_3$ peak in HA to the -CH_3 peak in the octadecyl group in the ^{1}H NMR spectrum of ALN-HA-C_{18} was calculated.[25] The DS of the octadecyl group in the ALN-HA-C_{18} polymer was 13.11%. The DS of ALN in the ALN-HA-C_{18} polymer determined by the potentiometric titration method was about 5.6%.

The CMC of the ALN-HA-C_{18} polymer

The CMC is an important parameter affecting the aggregation behavior of polymer micelles in solution, which can influence the self assembled ability of the amphiphilic polymer and the structural ability of micelles in vitro and in vivo.[26] The CMC of the ALN-HA-C_{18} polymer in aqueous solution was determined by fluorescence spectroscopy using pyrene as a hydrophobic fluorescence probe. Figure 3 shows the change in the fluorescence intensity ratio of I_{373}/I_{384} (I_1/I_3) against the logarithm of the ALN-HA-C_{18} polymer concentration and the CMC was estimated from the threshold concentration of the self assembled micelles. The ALN-HA-C_{18} copolymer had a low CMC value (10.8 μg/mL), which is significantly lower than traditional low molecular weight surfactants.[27] The low CMC value indicates that a better structural integrity can be obtained at a low polymer concentration and the micelles possessed better structural stability in vitro and in vivo.

Optimization of the preparation process

Taking particle size and EE% as the index, a series of preliminary screening experiments were first conducted in order to select the control factors, which significantly influenced the preparation process. The results indicated that particle size and EE% had obvious changes along with varying the mass ratio of polymer to drug, type of organic solvent, and solidification temperature. Therefore, these three factors were considered as variables for optimization through an orthogonal design L9 at three experimental levels. The mass ratio of polymer to drug was X_1 ranging from 5: 1 to 15: 1, the type of organic solvent was X_2 as chosen from ethanol, acetone, and chloroform, and the solidification temperature was X_3 in the range from 40 °C to 80 °C. The experimental design and results are shown in Table 2.

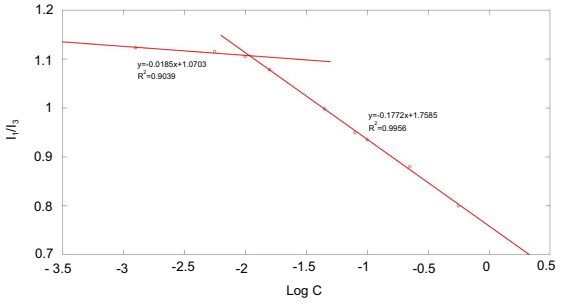

Figure 3 Plots of I_1/I_3 against the logarithim of the ALN-HA-C_{18} concentration.

The data was analyzed with SPSS 19.0 statistical software. The extreme difference (R) reflects the change range of the test index when the level of the variable factor fluctuates. A larger R means a greater influence of this factor on the test index. According to the analysis, the R and R', the order of influence for each factor on particle size and EE% was $X_3 > X_2 > X_1$. K is the average of the sum of the experimental indicators corresponding to the level of these factors. The optimum level and combination of these factors can be judged by the value of K. Considering a lower particle size and higher EE%, the final optimal results are as follows: the ratio of polymer to drug is 10: 1, the organic solvent for film formation is ethanol, and the solidification temperature of the film is 80 °C.

Preparation and characterization of CUR loaded ALN-HA-C_{18} micelles

Depending on the solubility and swelling property of the modified polysaccharides in water, micelles of hydrophobized polysaccharides can be prepared by a variety of methods, including a film dispersion method, dialysis, ultrasound, and emulsification. In this work, CUR loaded ALN-HA-C_{18} micelles were prepared by the film dispersion method. Micelles were formed by self-assembly whereby the ALN-HA-C_{18} polymer and CUR were dissolved in ethanol; then, a vacuum rotary evaporator was used to form a dried film followed by consolidating the film. The obtained film was dispersed into deionized water to obtain a micellar solution. In aqueous solution, hydrophobic interactions between grafted octadecyl chains contributed to form the self-assembled micelles and the hydrophobic octadecanoic acid aggregated together to form the micelle core. The hydrophilic HA backbone served as the shell of polymeric micelles responsible for providing an effective steric protection layer.[28]

The particle size and size distribution of the CUR loaded ALN-HA-C_{18} micelles are shown in Figure 4A.

Table 2 The orthogonal design L9 (3^4) and resulting values

Experiments	Variables			Responses	
	X_1: Polymer to drug	X_2: Type of organic solvent	X_3: Solidification temperature (°C)	Y_1: Particle size (nm)	Y_2: EE% (%)
1	1	1	1	244.4	12.3
2	1	2	2	248.5	37.6
3	1	3	3	324.2	9.7
4	2	1	2	122.2	36.6
5	2	2	3	115.3	34.4
6	2	3	1	472.5	8.2
7	3	1	3	200.8	18.0
8	3	2	1	220.2	32.3
9	3	3	2	377	10.8
K_1	272.4	189.1	312.4		
K_2	236.7	188.2	249.2		
K_3	266	391.2	213.4		
R	35.7	202.1	99		
K_1'	19.9	22.3	17.6		
K_2'	26.4	34.8	28.3		
K_3'	20.4	16.7	20.7		
R'	6.5	18.1	10.7		

The CUR loaded ALN-HA-C_{18} micellar average size was approximately 118 nm with a narrow size distribution. The particle size of the CUR loaded ALN-HA-C_{18} micelles was in a suitable size range for accumulating in tumor tissue by the enhanced permeability and retention (EPR) effect.[29] TEM images of the CUR loaded ALN-HA-C_{18} micelles are presented in Figure 4B, showing a spherical micellar nanoaggregate with uniform size and core-shell structures. However, the size estimated from the TEM images was smaller than that from DLS due to different sample preparation methods. It is conceivable that removal of water during the TEM sample drying process may have contributed to the shrinkage of the hydrophilic HA shell of the micelles.[30] Nevertheless, size determination by DLS was performed using the aqueous condition with an intact shell. Moreover, the CUR loaded ALN-HA-C_{18} micelles showed high drug loading with a DL% of about 6%. This was because the CUR was tightly wrapped in a hydrophobic core. Drug loading capacity is very important for the drug delivery system. Thus, a high DL% was very important for CUR loaded ALN-HA-C_{18} micelles.

In vitro release study

The drug release behavior of the free CUR and CUR loaded ALN-HA-C_{18} micelles were investigated in PBS (pH 5.7) containing 1% Tween 80 at 37 °C. As shown in Figure 4C, the free CUR released about 95% after 8 h. However, the CUR loaded ALN-HA-C_{18} micelles released 94% of CUR after 72 h. Compared to the rapid release of free CUR, the CUR loaded ALN-HA-C_{18} micelles had a two-step release pattern without a burst effect, indicating an initial rapid release period at 12 h, in which about 74% CUR was released, followed by a prolonged release of up to 72 h reaching a cumulative release of CUR close to 94%. It was, thus, obviously demonstrated that the release of CUR from the polymeric micelles was in a sustained manner, due to the hydrophobic core of micelles strongly restricting the migration of CUR into the release medium.[28]

Hydroxyapatite affinity assay

High affinity to bone tissue is the first requirement for bone targeted drug delivery. Meanwhile, for tumor metastasized bone tissue, the main composition of skeletal hydroxyapatite is exposed in lysed components.[31] Thus, the affinity of ALN-HA-C_{18} micelles to hydroxyapatite was quantitatively analyzed using hydroxyapatite powder. The binding ratios of CUR, CUR loaded HA-C_{18} micelles, and CUR loaded ALN-HA-C_{18} micelles are showed in Figure 4D. Most (79.8%) of the CUR loaded ALN-HA-C_{18} micelles bound to the hydroxyapatite powder, whereas only small amounts of CUR (12.5%) and CUR loaded HA-

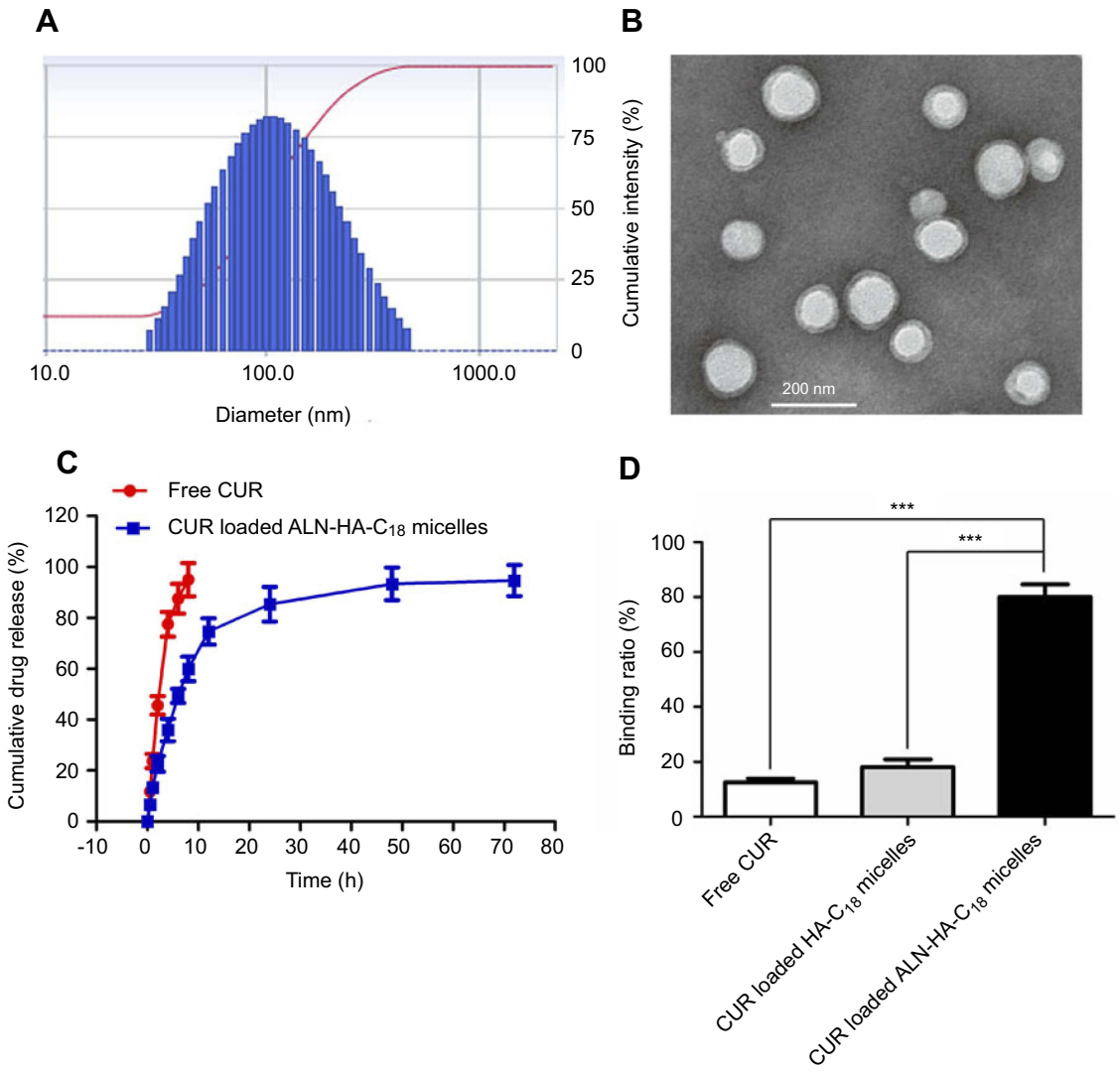

Figure 4 The size distribution (**A**) and transmission electron microscopy (TEM) image (**B**) of CUR loaded ALN-HA-C_{18} micelles. (**C**) In vitro release characteristics of free CUR and CUR loaded ALN-HA-C_{18} micelles in 1% Tween 80 PBS medium. (**D**) Binding ratio of CUR, CUR loaded HA-C_{18} micelles, and CUR loaded ALN-HA-C_{18} micelles with hydroxyapatite. Data are presented as the mean ± SD (n=3). ***Significant difference between the two groups (***$P<0.001$).

C_{18} micelles (17.6%) were adsorbed. CUR loaded ALN-HA-C_{18} micelles exhibited a significantly higher binding ratio (***$P<0.001$) than CUR and CUR loaded HA-C_{18} micelles, which was attributed to the ALN modification of the ALN-HA-C_{18} micelles. It has been well documented that ALN has a strong affinity with bone tissue due to its phosphonate and hydroxyl groups.[32] The above results implied that CUR loaded ALN-HA-C_{18} micelles could quickly accumulate at bone sites.

In vitro cytotoxicity assay

The in vitro cytotoxicity of CUR loaded ALN-HA-C_{18} micelles was assessed on MG-63 osteosarcoma cells and HOB cells with free CUR (CUR dissolution in DMSO) as a control. Blank ALN-HA-C_{18} micelles with the same copolymer concentrations as CUR loaded ALN-HA-C_{18} micelles were used as controls as well. The cells were incubated for 48 h in the presence of the test solutions, and then their survival was analyzed using an MTT assay.

The viability of HOB and MG-63 cells after incubation with blank micelles and various formulations of CUR are presented in Figure 5A and B. The blank micelles did not show obvious toxicity even at the highest concentration of 40 μM, indicating that the blank ALN-HA-C_{18} micelles could guarantee security. However, free CUR and CUR loaded ALN-HA-C_{18} micelles exhibited significant higher ($P<0.001$) cytotoxicity than blank micelles at a high CUR concentration exceeding 20 μM. On the other hand, CUR loaded ALN-HA-C_{18} micelles showed a similar inhibitory effect to free CUR in healthy HOB cells (Figure 5A).

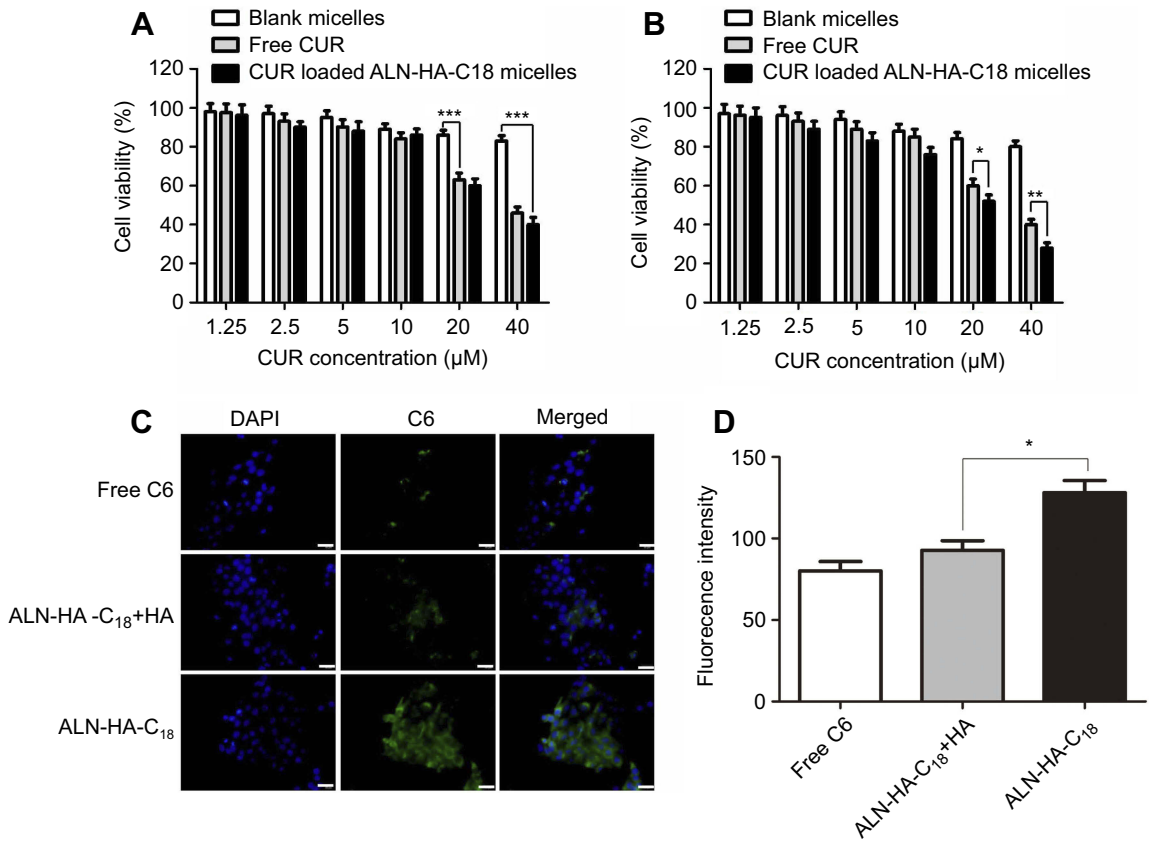

Figure 5 In vitro cytotoxicity of blank ALN-HA-C_{18} micelles, free CUR, and CUR loaded ALN-HA-C_{18} micelles against HOB cells (**A**) and MG-63 osteosarcoma cells (**B**). Fluorescence microscope images (**C**) and flow cytometry analysis (**D**) of MG-63 cells incubated with free C6, C6 loaded ALN-HA-C_{18} micelles with HA and C6 loaded ALN-HA-C_{18} micelles. Data are presented as the mean ± SD (n=6). *, ** and *** represent $P<0.05$, $P<0.01$ and $P<0.001$, respectively. The bar is 50 μm.

Additionally, the cellular inhibition of CUR loaded ALN-HA-C_{18} micelles was much greater than that by free CUR micelles for osteosarcoma MG-63 cells (Figure 5B), implying a targeting ability of CUR loaded ALN-HA-C_{18} micelles due to the affinity between HA and CD44 receptors on the MG-63 cell membrane. Accordingly, comparing to the passive diffusion of free CUR through the cell membrane, the higher cytotoxicity of CUR loaded ALN-HA-C_{18} micelles could be explained by a stronger binding affinity of HA to CD44 receptors and enhanced cellular uptake via CD44-mediated endocytosis in MG-63 cells.

Cellular uptake of micelles

In this experiment, coumarin 6 was used as a fluorescence marker. As shown in Figure 5C, there was little green C6 fluorescence in the cytoplasm and the nucleus of the MG-63 cells when the cells were incubated with the free C6 solution for 4 h. While, after MG-63 cells were incubated with C6 loaded ALN-HA-C_{18} micelles for 4 h, green C6 fluorescence intensity in the cytoplasm was strong and the green C6 fluorescence almost localized around the blue nucleus of the MG-63 cells. This result indicated that C6 loaded ALN-HA-C_{18} micelles were taken up efficiently by MG-63 cells, and C6 was released from ALN-HA-C_{18} micelles. On the other hand, the fluorescence intensity of C6 loaded ALN-HA-C_{18} micelles was much stronger than those of micelles in the presence of free HA for the MG-63 cells, which might be attributed to endocytosis mediated by the CD44 receptor.

The cellular uptake of C6 loaded ALN-HA-C_{18} micelles by MG-63 cells was further evaluated by flow cytometry. The result is shown in Figure 5D. It revealed that MG-63 cells following 4 h of incubation with C6 loaded ALN-HA-C_{18} micelles had higher fluorescence intensity than C6 loaded ALN-HA-C_{18} micelles with HA ($P<0.05$), which is consistent with inverted fluorescence microscope assays results and confirmed an active targeting ability of ALN-HA-C_{18} micelles.

In vivo antitumor activity

In order to evaluate the antitumor activity of CUR loaded ALN-HA-C_{18} micelles, the in vivo antitumor experiment was performed in osteosarcoma (MG-63 cells) models.

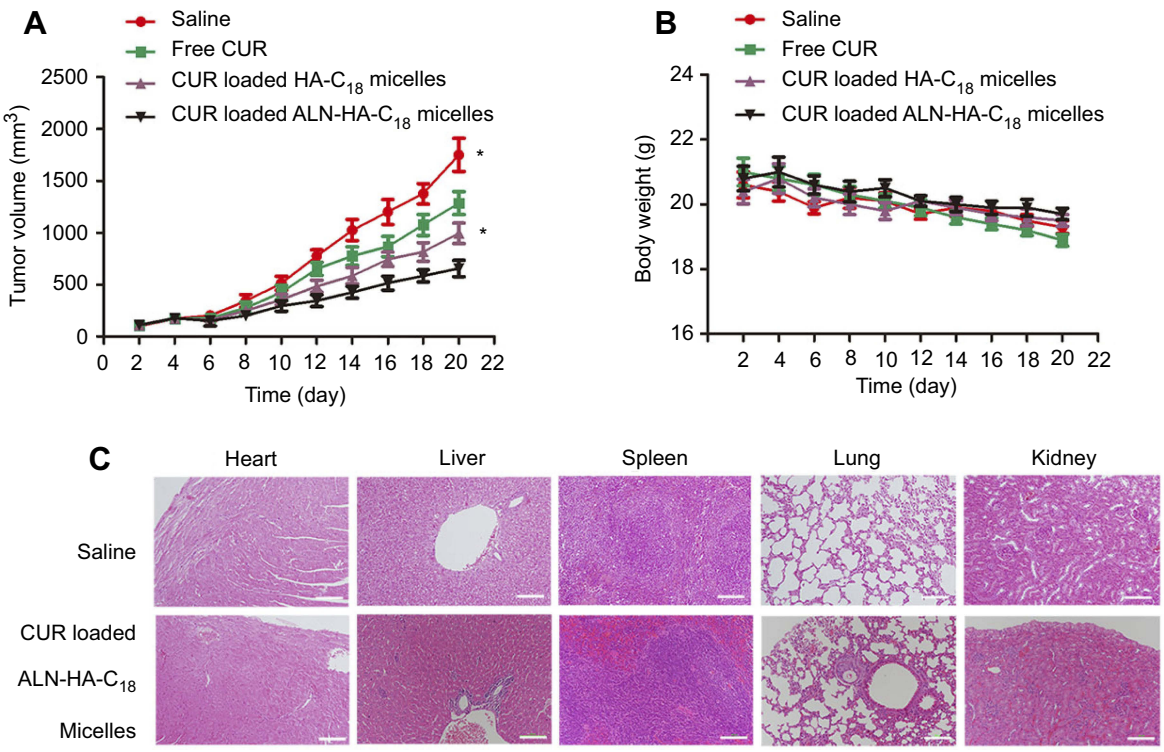

Figure 6 The in vivo antitumor activity of CUR loaded ALN-HA-C_{18} micelles on osteosarcoma bearing nude mice. (**A**) Tumor volume changes; and (**B**) body weight changes. (**C**) The hematoxylin and eosin (H&E) staining of the heart, liver, spleen, lung and kidney in saline and CUR loaded ALN-HA-C_{18} micelles group after treatment. Data are presented as the mean ± SD (n=6). *Represents $P<0.05$. Bars =100 μm.

After the injection of saline, free CUR, CUR loaded HA-C_{18} micelles and CUR loaded ALN-HA-C_{18} micelles into the tail vein, the tumor volume of mice was measured for 20 days. As shown in Figure 6A, the saline group did not show any regression effect on tumor growth, but the free CUR and CUR loaded HA-C_{18} micelles treatment exhibited obvious tumor growth inhibition ($P<0.05$) in vivo as compared with the saline group. When the tumor bearing nude mice were treated with CUR loaded ALN-HA-C_{18} micelles, tumor growth was significantly delayed ($P<0.05$) as compared with CUR loaded HA-C_{18} micelle treated mice. These results suggest that the CUR loaded ALN-HA-C_{18} micelle group exhibited the highest anti-tumor therapeutic efficacy among the groups proving that the CUR loaded ALN-HA-C_{18} micelles could target osteosarcoma and improve the curative effect of the hydrophobic drugs. In this case, some synergistic therapies such as photothermal therapy, photodynamic therapy and radiotherapy could be utilized in the future to inhibit tumor growth and further promote therapeutic efficiency.

An adverse effect is one of the major concerns in the research and development of novel drug delivery systems. The change in body weight of the tumor bearing nude mice is an important indication to evaluate systemic side effects.[31] As shown in Figure 6B, no obvious body weight loss was observed for the CUR loaded ALN-HA-C_{18} micelle treated mice. The tumor bearing nude mice treated with CUR loaded ALN-HA-C_{18} micelles kept a vigorous appearance throughout the full experiment. As shown in Figure 6C, H&E staining was used to observe histological alterations in the saline and CUR loaded ALN-HA-C_{18} micelle groups for different organs, including the heart, liver, spleen, lung and kidney. No significant organ change was observed for the CUR loaded ALN-HA-C_{18} micelle group, indicating the safety of the CUR loaded ALN-HA-C_{18} micelles.

The above results demonstrate that CUR loaded ALN-HA-C_{18} micelles could act as an ideal nano delivery system to deliver CUR into osteosarcoma cells with less systemic toxicity.

Conclusion

In the present study, we developed a dual targeting delivery system with ALN-HA-C_{18} micelles for the physical encapsulation of CUR. The newly developed nanomicellar systems had excellent performance features characterized with suitable particle size, high drug loading, sustained release, and high binding affinity with hydroxyapatite. CUR loaded

ALN-HA-C_{18} micelles could deliver more CUR into osteosarcoma tissue, which greatly improved in vivo antitumor activity with less systemic toxicity. Thus, this study suggested that CUR loaded ALN-HA-C_{18} micelles could be useful for bone applications and with CD44 receptor dual targeting, these nanocarriers should be further studied for the treatment of osteosarcoma.

Acknowledgments

This work was supported by the National Natural Science Foundation of China (Grant no. 81472071 and Grant no. 81301537), Shanghai Science and Technology Committee Scientific Research Plan Project (Grant no. 12nm0501202), the Shanghai Changzheng Hospital Foundation (Grant no. 2017CZQN05), Natural Science Foundation of Shanghai, (No. 19ZR1456800), Youth Medical Talent Project of Jiangsu (QNRC2016214), Key Technologies of Prevention and Control for Major and Infectious Diseases (No. GWZX201604), and Project of Science and Technology of Changshu Health Commission (csws201714).

Disclosure

The authors report no conflicts of interest in this work.

References

1. Nabavi SF, Daglia M, Moghaddam AH, Habtemariam S, Nabavi SM. Curcumin and liver disease: from chemistry to medicine. *Compr Rev Food Sci Food Saf*. 2013;13(1):62–77.
2. Aggarwal BB, Kumar ABharti AC. Anticancer potential of curcumin: preclinical and clinical studies. *Anticancer Res*. 2003;23(1A):363–398.
3. Steward WP, Gescher AJ. Curcumin in cancer management: recent results of analogue design and clinical studies and desirable future research. *Mol Nutr Food Res*. 2010;52(9):1005–1009. doi:10.1002/mnfr.200700148
4. Lin JK, Lin-Shiau SY. Mechanisms of cancer chemoprevention by curcumin. *Proc Natl Sci Counc Repub China B*. 2001;25(2):59–66.
5. Leung MHM, Hannah C, Kee TW. Encapsulation of curcumin in cationic micelles suppresses alkaline hydrolysis. *Langmuir*. 2008;24(11):5672–5675. doi:10.1021/la800780w
6. Sahu A, Bora U, Kasoju N, Goswami P. Synthesis of novel biodegradable and self-assembling methoxy poly(ethylene glycol)–palmitate nanocarrier for curcumin delivery to cancer cells. *Acta Biomater*. 2008;4(6):1752–1761. doi:10.1016/j.actbio.2008.04.021
7. Bisht S, Feldmann G, Soni S, et al. Polymeric nanoparticle-encapsulated curcumin ("nanocurcumin"): a novel strategy for human cancer therapy. *J Nanobiotechnology*. 2007;5(1):3. doi:10.1186/1477-3155-5-3
8. Li L, Ahmed B, Mehta K, Kurzrock R. Liposomal curcumin with and without oxaliplatin: effects on cell growth, apoptosis, and angiogenesis in colorectal cancer. *Mol Cancer Ther*. 2007;6(4):1276–1282. doi:10.1158/1535-7163.MCT-06-0556
9. Praveen Kumar V, Jun L, George J. Enzyme catalysis: tool to make and break amygdalin hydrogelators from renewable resources: a delivery model for hydrophobic drugs. *J Am Chem Soc*. 2006;128(27):8932–8938. doi:10.1021/ja062650u
10. Tonnesen HH. Solubility, chemical and photochemical stability of curcumin in surfactant solutions. Studies of curcumin and curcuminoids, XXVIII. *Pharmazie Die*. 2002;57(12):820–824.
11. Chignell CF, Bilski P, Reszka KJ, Motten AG, Sik RH, Dahl TA. Spectral and photochemical properties of curcumin. *Photochem Photobiol*. 2010;59(3):295–302. doi:10.1111/j.1751-1097.1994.tb05037.x
12. Laurent TC. Biochemistry of Hyaluronan. *Acta Otolaryngol*. 2009;104(sup442):7–24. doi:10.3109/00016488709102833
13. Herrlich P, Sleeman J, Wainwright D, et al. How tumor cells make use of CD44. *Cell Adhes Commun*. 1998;6(2–3):141. doi:10.3109/15419069809004470
14. Hall CL, Yang B, Yang X, et al. Overexpression of the hyaluronan receptor RHAMM is transforming and is also required for H-ras transformation. *Cell*. 1995;82(1):19–26. doi:10.1016/0092-8674(95)90048-9
15. Lee H, Mok H, Lee S, Oh YK, Park TG. Target-specific intracellular delivery of siRNA using degradable hyaluronic acid nanogels. *J Control Release*. 2007;119(2):245–252. doi:10.1016/j.jconrel.2007.02.011
16. Larsen NE, Balazs EA. Drug delivery systems using hyaluronan and its derivatives. *Adv Drug Deliv Rev*. 1991;7(2):279–293. doi:10.1016/0169-409X(91)90007-Y
17. Maya K, Teng MW, Smyth MJ, Thomas DM. Translational biology of osteosarcoma. *Nat Rev Cancer*. 2014;14(11):722–735. doi:10.1038/nrc3838
18. Botter SM, Neri D, Fuchs B. Recent advances in osteosarcoma. *Curr Opin Pharmacol*. 2014;16(1):15–23. doi:10.1016/j.coph.2014.02.002
19. Arndt CA, Crist WM. Common musculoskeletal tumors of childhood and adolescence. *N Engl J Med*. 2012;87(5):475–487.
20. Neyssa M, Mark G, Lisa T, Richard G. Biology and therapeutic advances for pediatric osteosarcoma. *Oncologist*. 2004;9(4):422. doi:10.1634/theoncologist.9-4-422
21. Bielack SS, Beate KB, Günter D, et al. Prognostic factors in high-grade osteosarcoma of the extremities or trunk: an analysis of 1,702 patients treated on neoadjuvant cooperative osteosarcoma study group protocols. *Hum Cell*. 2004;17(3):131–137.
22. Tianling C, James B, Robert V, et al. Pharmacokinetics and pharmacodynamics of zoledronic acid in cancer patients with bone metastases. *J Clin Pharmacol*. 2013;42(11):1228–1236.
23. Pan H, Sima M, Kopecková P, et al. Biodistribution and pharmacokinetic studies of bone-targeting N-(2-hydroxypropyl)methacrylamide copolymer-alendronate conjugates. *Mol Pharm*. 2008;5(4):548–558. doi:10.1021/mp800003u
24. Uludag H. Bisphosphonates as a foundation of drug delivery to bone. *Curr Pharm Des*. 2002;8(21):1924–1944.
25. Hyukjin L, Cheol-Hee A, Tae Gwan P. Poly[lactic-co-(glycolic acid)]-grafted hyaluronic acid copolymer micelle nanoparticles for target-specific delivery of doxorubicin. *Macromol Biosci*. 2010;9(4):336–342.
26. Qiu L, Li Z, Qiao M, et al. Self-assembled pH-responsive hyaluronic acid-g-poly((L)-histidine) copolymer micelles for targeted intracellular delivery of doxorubicin. *Acta Biomater*. 2014;10(5):2024–2035. doi:10.1016/j.actbio.2013.12.025
27. Cho H-J, Yoon HY, Koo H, et al. Self-assembled nanoparticles based on hyaluronic acid-ceramide (HA-CE) and Pluronic? For tumor-targeted delivery of docetaxel. *Biomaterials*. 2011;32(29):7181–7190. doi:10.1016/j.biomaterials.2011.06.028
28. Liu Y, Sun J, Cao W, et al. Dual targeting folate-conjugated hyaluronic acid polymeric micelles for paclitaxel delivery. *Int J Pharm*. 2011;421(1):160–169. doi:10.1016/j.ijpharm.2011.09.006
29. Iyer AK, Khaled G, Fang J, Maeda H. Exploiting the enhanced permeability and retention effect for tumor targeting. *Drug Discov Today*. 2006;11(17):812–818. doi:10.1016/j.drudis.2006.07.005
30. Jing L, Meirong H, Jing W, et al. Redox-sensitive micelles self-assembled from amphiphilic hyaluronic acid-deoxycholic acid conjugates for targeted intracellular delivery of paclitaxel. *Biomaterials*. 2012;33(7):2310–2320. doi:10.1016/j.biomaterials.2011.11.022

31. Ye WL, Zhao YP, Li HQ, et al. Doxorubicin-poly (ethylene glycol)-alendronate self-assembled micelles for targeted therapy of bone metastatic cancer. *Sci Rep*. 2015;5:14614. doi:10.1038/srep14614

32. Ozcan I, Bouchemal K, Segura-Sánchez F, Ozer O, Güneri T, Ponchel G. Synthesis and characterization of surface-modified PBLG nanoparticles for bone targeting: in vitro and in vivo evaluations. *J Pharm Sci*. 2011;100(11):4877–4887. doi:10.1002/jps.22678